

# Electromechanical Behavior of $\text{Bi}_2\text{Sr}_2\text{CaCu}_2\text{O}_x$ Conductor Using a Split Melt Process for React-Wind-Sinter Magnet Fabrication

Tengming Shen, Xiaotao Liu, Ulf Peter Trociewicz, and Justin Schwartz, *Fellow, IEEE*

**Abstract**—A new approach to magnet fabrication, react, wind and sinter (RWS), has been proposed for  $\text{Bi}_2\text{Sr}_2\text{CaCu}_2\text{O}_x$  (Bi2212), magnets. In this process, the conventional Bi2212 heat treatment is split into two portions, and the magnet is wound between these heat treatments. Here we report results on the RWS “split melt process”. Significant increases in  $J_c$  are obtained in Bi2212 round wires compared to standard melt processing. Strain effect measurements, using the Lorentz force, indicate that RWS wires have similar mechanical performance as wind and react wires. Effects of the split melt temperature on the electromechanical properties are also reported. These results show that split melt processing and RWS magnet fabrication are viable approaches for Bi2212 conductors and magnets.

**Index Terms**—Bi2212, superconducting magnet.

## I. INTRODUCTION

**B** $\text{i}_2\text{Sr}_2\text{CaCu}_2\text{O}_x$  (Bi2212) conductor has very high critical current density,  $J_c$ , at low temperature and high magnetic field, and thus is very attractive for high field applications. Compared to other high temperature superconductors, Bi2212 is particularly attractive because it is available as a round wire. Potential applications include insert magnets for 30 T NMR magnets [1] and high field accelerator magnets [2], [3]. Research continues to improve the current-carrying capability of Bi2212 round wire; practical Bi2212 wire now has an engineering critical current density,  $J_e$ , of at least  $380 \text{ A/mm}^2$ , at 4.2 K and 25 T [4].

Bi2212 is a brittle ceramic, becoming highly strain sensitive [5]–[7] after final processing at high temperature. This strongly influences the options for magnet fabrication. Traditionally, there are two approaches to superconducting magnet fabrication: Wind and React (W&R) and React and Wind (R&W). R&W is more suitable for thin tape conductors [8] since the bending strain on round wire would be much larger for equal

Manuscript received August 26, 2007. This work was supported by the U.S. National Institute of Health SBIR Phase II Grant through Supercon, Inc.

T. Shen is with National High Magnetic Field Laboratory, Florida State University, Tallahassee, FL 32310, and also with the Department of Electrical and Computer Engineering at the FAMU-FSU College of Engineering, Tallahassee, FL 32310 USA.

X. Liu and U. P. Trociewicz are with National High Magnetic Field Laboratory, Florida State University, Tallahassee, FL 32310 USA.

J. Schwartz is with National High Magnetic Field Laboratory, Florida State University, Tallahassee, FL 32310, and also with the Department of Mechanical Engineering at the FAMU-FSU College of Engineering, Tallahassee, FL 32310 USA (e-mail: Schwartz@magnet.fsu.edu).

Color versions of one or more of the figures in this paper are available online at <http://ieeexplore.ieee.org>.

Digital Object Identifier 10.1109/TASC.2008.921360

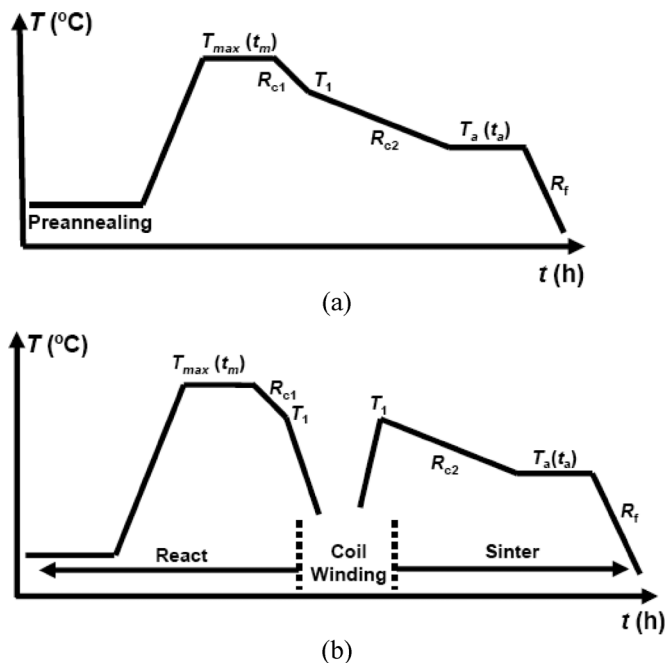


Fig. 1. (a) Typical melt processing and (b) split melt processing schedules for Bi2212 conductors and magnets [10].

bending radius and would limit the current carrying ability or the available strain margin.

Recent coils with Bi2212 round wire have used W&R [9]. The coil is wound when conductor is still ductile and the bending strain is relieved during the partial melt heat treatment. Other factors related to the partial-melt heat treatment inherent to Bi2212 processing, however, hinder the application of W&R fabrication for large high field magnets.

The partial-melt process (MP) typically used on oxide power-in-tube Bi2212 wires is shown in Fig. 1(a). It consists of heating conductor above the peritectic decomposition temperature of the Bi2212 phase and slowly cooling down to form a well-connected and aligned Bi2212 grain structure. Some essential factors of MP make W&R difficult.

The MP typically requires pure  $\text{O}_2$  and a peak processing temperature of  $\sim 890^\circ\text{C}$  for a short period of time (typically  $\sim 12$  minutes). The microstructure of Bi2212 is extremely sensitive to both peak temperature and the time at this temperature and high  $J_c$  is obtained in a small processing window. As the phase assemblages in the oxides vary with oxygen content, both oxygen and thermal diffusion can limit the magnet size that can be uniformly heat treated. Furthermore, the selection of

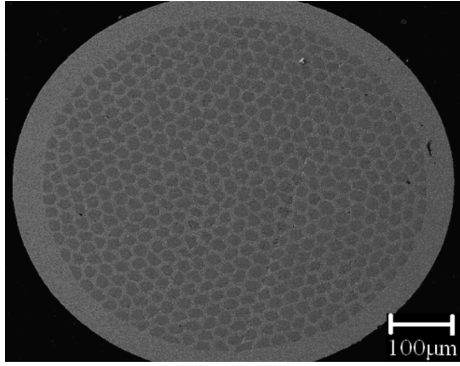


Fig. 2. Cross section of a 0.8 mm multifilamentary Bi2212 wire before heat treatment. The wire has 521 filaments with an average size of around  $20\ \mu\text{m}$ .

turn-to-turn insulation is difficult. Lastly, tightly wound Bi2212 W&R coils often encounters problems with ceramic leakage, where the liquid phase often penetrates the surrounding Ag alloy matrix and reacts with the insulation. The intertwined complications of the narrow processing window, insulation, leakage and chemical reactions may explain why some recent W&R coils have only performed at 60% of short sample  $J_c$  [4], [9].

An alternative approach to magnet fabrication, React-Wind-Sinter (RWS), has recently been proposed [10] to overcome the problems associated with both W&R and R&W (Fig. 1(b)). In this process, the conventional Bi2212 heat treatment is split into two separate heat treatments and the magnet is wound between them. The assumption is that the ceramic leakage and  $J_c$  sensitivity to peak temperature and soaking time are more critical in the liquid state. In the first heat treatment (HT1), loosely-wound long-length wire would be heat treated on a mandrel designed for heat treatment, facilitating precise temperature control and homogenous  $\text{O}_2$  diffusion. The coil would then be wound and go through the second heat treatment (HT2) with less concern about precise temperature control and oxygen diffusion.

The heat treatment schedule for RWS magnets, shown in Fig. 1(b), is referred to as split melt processing (SMP). Uncertainty with RWS first involves the question of whether SMP produces high  $J_c$  in Bi2212 conductor. Initial results [10] indicate that high performance is obtained. The split temperature, however, is expected to be an important parameter to be optimized. After HT1, the Bi2212 filaments may be strain sensitive as some Bi2212 phase has formed and winding may cause microcracks or fracture, destroying the integrity of grain connectivity. The role of HT2 is to grow Bi2212 grains into well-connected structures, eliminating the winding damage, and thus realize high  $J_c$ . Therefore, the second uncertainty concerns whether HT2 heals any bending effects, resulting in a coil with a similar strain-state as a W&R coil.

Here, we first investigated SMP on straight wire samples to determine the effects on  $J_c$ . We then added a bending step between heat treatments to emulate RWS processing and measured the electromechanical behavior.

## II. EXPERIMENTAL DETAILS

### A. Conductor

Fig. 2 shows the cross-section of the multifilamentary Bi2212/Ag-alloy round wire used in this study. The wire was

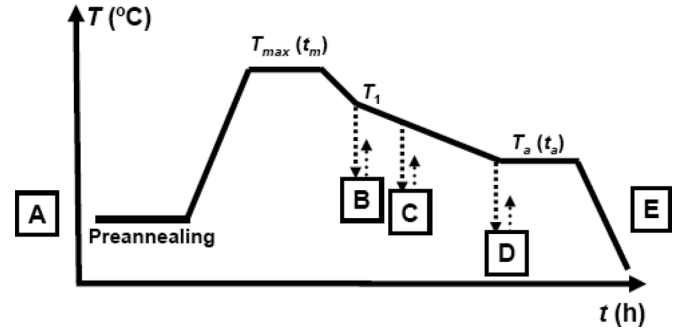


Fig. 3. RWS process split at various points of the heat treatment. Note that A is equivalent to W&R, E is equivalent to R&W, and the split temperatures for process B, C, and D are  $T_1$ ,  $T_1 - 15^\circ\text{C}$ , and  $T_a$  ( $T_1 - 47^\circ\text{C}$ ), where  $T_1 = T_{\text{max}} - 7^\circ\text{C}$ .

supplied by Supercon, Inc.; details of the wire processing are reported previously in [11].

### B. Heat Treatment

Heat treatment of 4.5 cm long straight samples was done in a three zone Lindberg tube furnace, with all samples located in a thermally homogeneous region. The temperature-time data was carefully monitored via Labview. A peak temperature variation within  $0.5^\circ\text{C}$  was obtained to assure reproducibility. The ends of the wire were mechanically sealed before heat treatment to avoid ceramic leakage.

Samples were processed using the following temperature-time process: ramp from room temperature to  $820^\circ\text{C}$  at  $160^\circ\text{C/h}$ , hold for 2 h, heat to the peak temperature ( $T_{\text{max}}$ ,  $885\text{--}895^\circ\text{C}$ ), hold for 12 minutes, cool at  $10^\circ\text{C/h}$  to  $T_1 (= T_{\text{max}} - 7^\circ\text{C})$ , cool at  $1\text{--}2.5^\circ\text{C/h}$  to  $833^\circ\text{C}$ , hold for 21–48 hours, and finally furnace cool to room temperature ( $\sim 85$  hours).

SMP was realized by interrupting the above process at a split temperature,  $T_s$ , cooling to room temperature, and then reheating to  $T_s$  to complete the process.  $T_s$  is an important processing variable; in this study,  $T_s = T_1$  unless otherwise stated.

### C. Heat Treatment of Bent Samples to Emulate RWS

The RWS fabrication process was emulated in short samples by heat treating wires bent into a machined macor bending rig modified from our previous report [10]. The bending rig consists of eight grooves, accommodating eight samples with bending diameters (BD) varying from 30 mm to 100 mm. The bending rig holds the samples during heat treatment, thereby emulating the wire geometry in a coil during heat treatment.

### D. Effect of Split Temperature

To study the effects of varying  $T_s$  on the electrical and mechanical properties, a set of RWS samples was heat treated as shown in Fig. 3. For comparison, W&R (A) and R&W (E) samples were also processed. For each heat treatment process, samples were bent to diameters ranging from 30 mm to 100 mm.

### E. Electromechanical Property Measurements

To measure the effects of strain on bent samples without straightening them, we utilize a technique which employed the

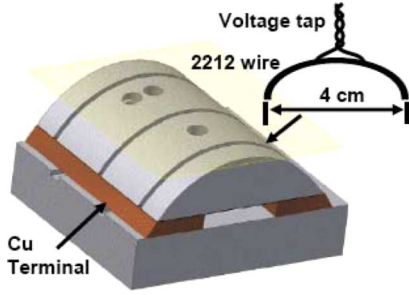


Fig. 4. Schematic view of the sample holder for electromechanical testing.

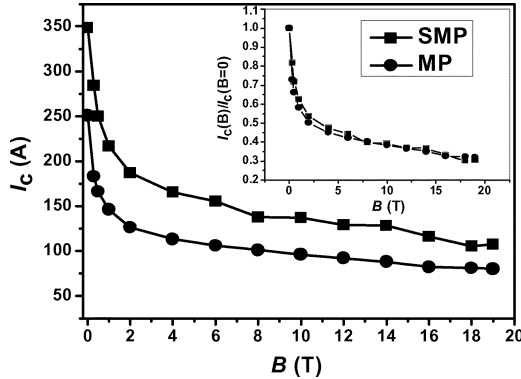


Fig. 5.  $I_c$  at 4.2 K as a function of magnetic field up to 19 T for two Bi2212 wires, one processed by MP and the other by SMP with  $T_s = T_1 = T_{\max} - 7^\circ\text{C}$ . The inset shows the same data normalized to the respective self-field  $I_{c0}$ .

Lorentz-force as mechanical load [12]. By reversing the polarity of the transport current in the sample, measurements are made both in compression and tension. The electromechanical testing device is shown in Fig. 4. It is comprised of a G-10 sample holder, Cu contacts and a supporting structure. After heat treatment, bent samples are laid into the grooves in the G-10 holder and soldered to the Cu. A set of G-10 sample holders with bending diameter from 30-100 mm was developed to match the bend diameters of the samples. The voltage-current characteristics were measured under two test modes in magnetic fields up to 19 T. In compression, the Lorentz force is pressing the sample into the G-10. In tension, the Lorentz force is pulling sample away from the G-10. Thus, in compression the sample is supported and in tension it is unsupported. The NHMFL large bore resistive magnet provided a magnetic field up to 19.3 T for this study. Note that the force applied is limited by the maximum field,  $I_c$ , and the bending radius.

The voltage-current characteristics were measured using the standard four probe method in liquid helium. The magnetic field was applied perpendicular to the axis of wire.  $I_c$  was extracted from the  $V - I$  curves using a  $1 \mu\text{V}/\text{cm}$  criterion.

### III. RESULTS

#### A. $I_c(B)$

Fig. 5 shows the  $I_c(B)$  of MP and SMP processed straight samples, showing that SMP increases performance by over 40% and does not affect the field dependence. In this experiment, the SMP used  $T_s = T_1$  (Process B in Fig. 3).

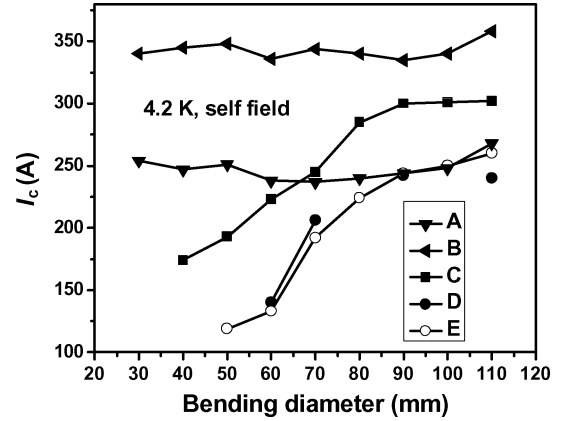


Fig. 6. Critical current as a function of bending diameter (inverse bending strain) for samples processed as shown in Fig. 3.

#### B. The Effect of Split Temperature

Fig. 6 shows the  $I_c$  dependence on bending diameter for the five sets of samples heat treated as shown in Fig. 3 with varying bending diameters. Comparison of  $I_c$  with a 110 mm bending diameter (original bending diameter of the as-received green wire) shows that various split heat treatments have higher  $I_c$  compared to standard melt processing, confirming the results in Fig. 5. When  $T_s$  approaches the melt temperature, higher  $I_c$  is achieved. The highest  $I_c$  was obtained with process B, which has the highest split temperature. Also important to note is that the process B samples show no decrease in  $I_c$  even with a 30 mm bending diameter, indicating RWS-B might have similar strain-state as W&R (Process A) samples. This implies that the SMP is capable of healing any damage to the Bi2212 filaments due to bending.

In addition, Fig. 6 shows that  $I_c$  of RWS processes C and D decreases as the bending diameter decreases, similar to R&W. Process D performance is almost identical to the R&W (Process E) sample. For process C, however, the dependence is not quite as strong (Fig. 7). This further implies that HT2 heals the strain damage from bending. It is unclear if the differences in strain tolerance of B, C and D are due to Bi2212 grain growth from the remnant unreacted liquid from HT1 or crack healing due to atomic diffusion. It is important to note, however, that HT2 of process B may involve the creation of some liquid phase, or is at least sufficiently close to the melting temperature of the unreacted remnant liquid from HT1 to provide enhanced atomic diffusion; this is a key factor for healing the mechanical defects that result from bending.

#### C. Lorentz Force Effects

Further electromechanical testing was performed on RWS-B samples to determine the mechanical state of the conductor by the method shown in Fig. 4. W&R conductors were tested for comparison.

The maximum hoop stress in tension mode during an individual test,  $\sigma$ , is determined from

$$\sigma = J_e \times B \times r \quad (1)$$

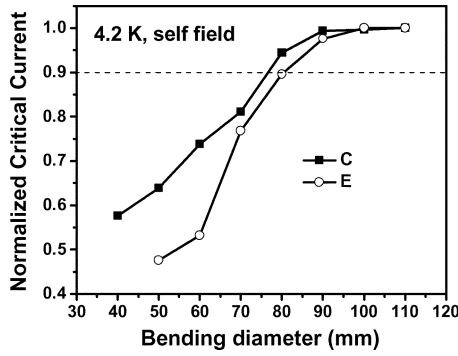


Fig. 7. Normalized critical current as a function of bending diameter for samples C and E.

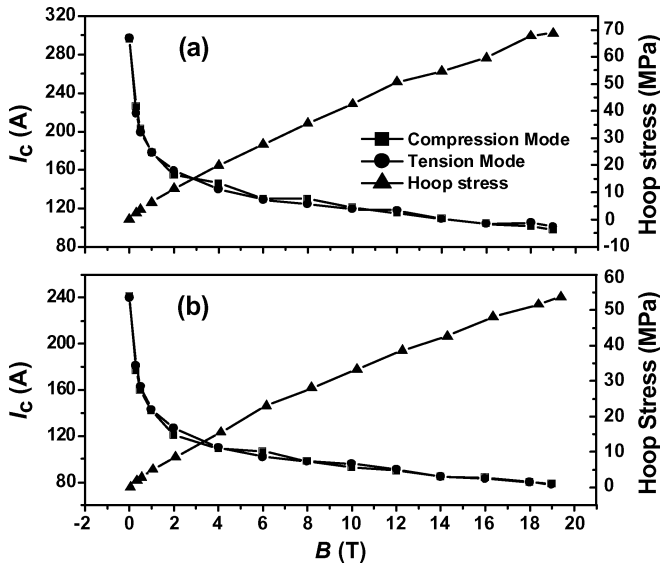


Fig. 8. Lorentz force effect on (a) RWS and (b) W&R samples with a bending diameter of 30 mm at 4.2 K. Also shown is the corresponding maximum hoop stress in tension mode.

where  $r$  is bending radius,  $J_e$  is the highest engineering current density during an individual test, and  $B$  is the background magnetic field. A group of samples were tested with bending diameters from 30 mm to 70 mm. The hoop stress increased with the bending diameter and magnetic field, reaching a maximum at over 200 MPa at 70 mm and 19 T.

Figs. 8–11 show the results of these experiments.  $I_c$  as a function of the background magnetic field, and the corresponding hoop stresses, are shown for W&R and RWS-B samples. Note that the maximum stress increases with increasing bend diameter. At a 30 mm bending diameter, the hoop stress was insufficient to cause degradation. W&R samples were also not degraded at 90 MPa (BD = 50 mm, Fig. 9(b)) but were degraded at 78 MPa (BD = 60 mm, Fig. 10(b)) and 87 MPa (BD = 70 mm, Fig. 11(b)). These differences are likely due to sample-to-sample variation that has been seen previously in  $\text{Bi}2212$  tapes [13]. RWS samples were degraded at 90 MPa (BD = 50 mm, Fig. 9(a)), 94 MPa (BD = 60 mm, Fig. 10(a)), and 105 MPa (BD = 70 mm, Fig. 11(a)). These results show that W&R and RWS samples degrade in the stress range of 85–110 MPa. It is difficult to be more precise due to the

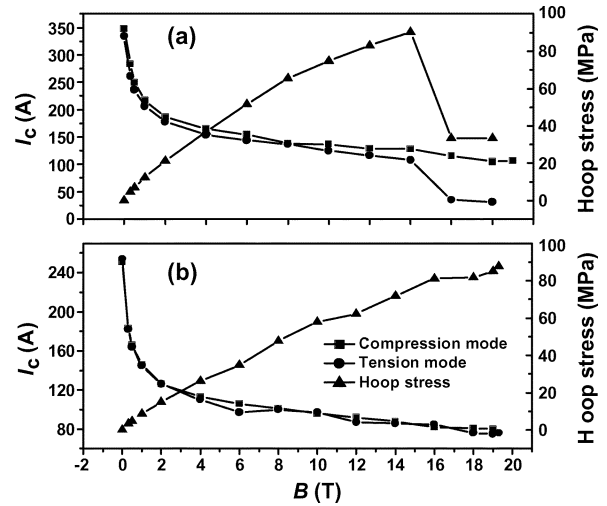


Fig. 9. Lorentz force effect on (a) RWS and (b) W&R samples with a bending diameter of 50 mm at 4.2 K.

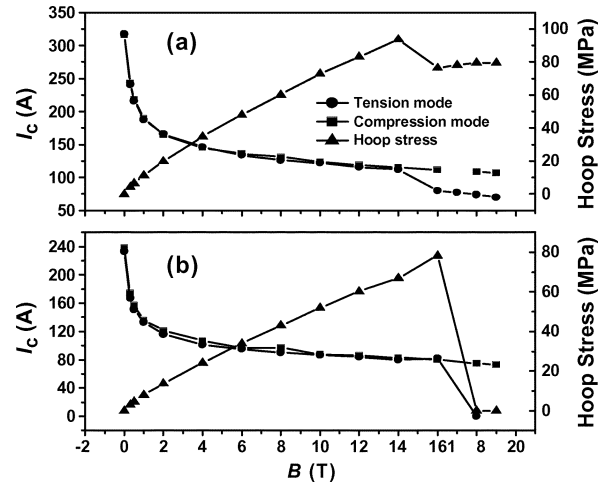


Fig. 10. Lorentz force effect on (a) RWS and (b) W&R samples with a bending diameter of 60 mm at 4.2 K.

sample-to-sample variations and because the Lorentz force technique is based in part on the measuring  $I_c$  while applying the load, so one does not have complete control over the amount of load applied. Furthermore, the calculated stress is the maximum within the cross-section, and thus an inhomogeneous current distribution in within the wire is not considered. These results indicate, however, that RWS-B wires are mechanically equivalent to W&R wires.

#### D. Differential Thermal Analysis

Differential thermal analysis was performed on an unreacted wire and one that experienced only HT1 ( $T_s = T_1$ ); results are shown in Fig. 12. It is seen that after HT1, the temperature at which melting begins is decreased by about 3°C. Thus it is possible that, even though  $T_s$  is below the solidification temperature initially, when returning to  $T_s$  at the beginning of HT2, some re-melting may occur. This may explain the significant difference in strain tolerance between heat treatments B and C seen in Fig. 6.

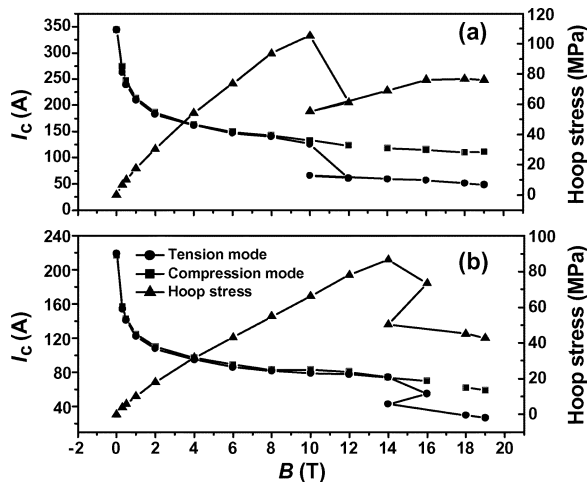


Fig. 11. Lorentz force effect on (a) RWS and (b) W&R samples with a bending diameter of 70 mm at 4.2 K.

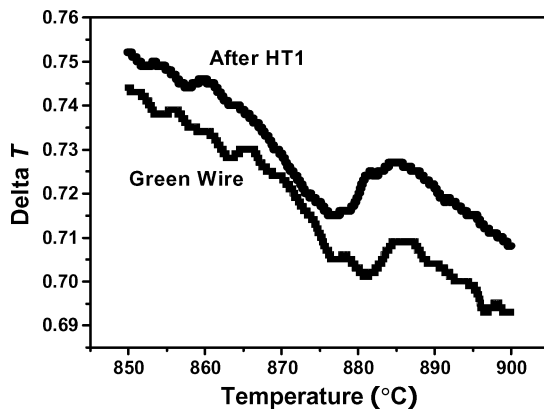


Fig. 12. Differential thermal analysis results for unreacted wire and a wire heat treated through HT1.

#### IV. DISCUSSION

The  $I_c$  enhancement by SMP poses the question as to whether the improvement is due to enhanced flux pinning or an improved microstructure, including reduced porosity, non-superconducting phases and enhanced connectivity. Fig. 5 shows that the field dependences of  $I_c$  of SMP and MP samples are nearly identical, indicating similar flux pinning properties. In general, Bi2212 wire performance is microstructure limited and this is where the improvements are likely to be found. Thus, further studies of the split melt processing, including detailed microstructural comparisons with MP samples, are expected to provide insight into current limiting factors in Bi2212 round wire. The SMP heat treatment schedule reported here is not considered optimum and further optimization is expected to improve  $J_c$ . It is clear, however, that RWS is viable alternative to W&R for net-shape magnet fabrication.

#### V. CONCLUSION

Split melt processing has resulted in a 40% increase in the  $J_c$  of Bi2212 round wires at 4.2 K, indicating that conventional Bi2212 wire processing is far from optimized. Many SMP parameters require further optimization which is likely to result in even greater performance enhancements. Furthermore, RWS processed wires are shown to match the mechanical performance of W&R wires, suggesting that an alternative to R&W and W&R can be developed that is tailored to the unique challenges of Bi2212 for high field magnets.

#### ACKNOWLEDGMENT

The authors thank Terence Wong and William Nachtrab of Supercon, Inc, for providing conductor and also Dr. Jianyi Jiang for helpful discussions.

#### REFERENCES

- [1] W. D. Markiewicz, J. R. Miller, J. Schwartz, U. P. Trociewitz, and H. W. Weijers, "Perspective on a superconducting 30 T/1.3 GHz NMR spectrometer magnet," *IEEE Trans. Appl. Supercond.*, vol. 16, no. 2, pp. 1523–1526, 2006.
- [2] P. J. Lee and D. Larbalestier, "Advances in superconducting strands for accelerator magnet application," in *Proc. of the 2003 Particle Accelerator Conference*, Portland, Or, May 12–16, 2003.
- [3] E. W. Collings, M. D. Sumption, R. M. Scanlan, D. R. Dietderich, L. R. Motosidlo, R. S. Sokolowski, Y. Aoki, and T. Hasegawa, "Bi-2212/Ag-based Rutherford cables: Production, processing and properties," *Supercon. Sci. Technol.*, vol. 12, pp. 87–96, 1999.
- [4] S. Hong, H. Miao, M. Meinesz, B. Czabaj, P. Noonan, A. Twin, R. Harrison, and K. Marken, "Bi-2212 wire & high field insert development," presented at the Low Temperature Superconductor Workshop, Tallahassee, FL, USA, November 2006, unpublished.
- [5] B. ten Haken, H. H. J. Ten Kate, and J. Tenbrink, "Compressive and tensile axial strain reduced critical currents in Bi-2212 conductors," *IEEE Trans. Appl. Supercond.*, vol. 5, no. 2, pp. 1298–1308, 1995.
- [6] B. ten Haken, A. Godeke, H.-J. Schuver, and H. H. J. ten Kate, "Descriptive model for the critical current as a function of axial strain in Bi-2212/Ag wire," *IEEE Trans. Magn.*, vol. 32, no. 4, pp. 2720–2723, 1996.
- [7] A. L. Mbaruku, K. R. Marken, M. Meinesz, H. Miao, P. V. P. S. S. Sastry, and J. Schwartz, "Effect of processing defects on stress-strain- $I_c$  for AgMg sheathed Bi-2212 tapes," *IEEE Trans. Appl. Supercond.*, vol. 13, no. 2, pp. 3522–3525, 2003.
- [8] H. W. Weijers, U. P. Trociewitz, K. Marken, M. Meinesz, H. Miao, and J. Schwartz, "The generation of 25.05 T using a 5.11 T BiSrCaCuO superconducting insert magnet," *Supercon. Sci. Technol.*, vol. 17, pp. 636–644, 2004.
- [9] H. Miao, K. R. Marken, M. Meinesz, B. Czabaj, S. Hong, A. Twin, P. Noonan, U. P. Trociewitz, and J. Schwartz, "High Field Insert Coils From Bi-2212/Ag Round Wires," *IEEE Trans. Appl. Supercond.*, vol. 17, no. 2, pp. 2262–2265, 2007.
- [10] J. Schwartz and G. A. Merritt, "Proof-of-principle experiments for react-wind-sinter manufacturing of  $\text{Bi}_2\text{Sr}_2\text{CaCu}_2\text{O}_x$  magnets," *Supercon. Sci. Technol.*, vol. 20, pp. L59–L62, 2007.
- [11] W. T. Nachtrab, M. K. Rudziak, and T. Wong, "Reactions between Bi-2212 and silver-nickel composite sheath," *IEEE Trans. Appl. Supercond.*, vol. 17, no. 2, pp. 3091–3094, 2007.
- [12] J. Schwartz, B. C. Amm, H. Garmestani, D. K. Hilton, and Y. Hascicek, "Mechanical properties and strain effects in  $\text{Bi}_2\text{Sr}_2\text{CaCu}_2\text{O}_x/\text{AgMg}$  composite conductors," *IEEE Trans. Appl. Supercond.*, vol. 7, no. 2, pp. 2038–2041, 1997.
- [13] A. L. Mbaruku and J. Schwartz, "Statistical analysis of electro-mechanical properties of AgMg sheathed  $\text{Bi}_2\text{Sr}_2\text{CaCu}_2\text{O}_{8+x}$  superconducting tapes using Weibull distributions," *J. Appl. Phys.*, vol. 101, no. 7, p. 073913, 2007.
- [14] K. Heine, J. Tenbrink, and M. Thöner, "High-field critical current densities in  $\text{Bi}_2\text{Sr}_2\text{Ca}_1\text{Cu}_2\text{O}_{8+x}/\text{Ag}$  wires," *Appl. Phys. Lett.*, vol. 55, no. 23, pp. 2441–2443, 1989.